J Porous Mater (2016) 23:431–440
DOI 10.1007/s10934-015-0097-4

# Covalent anchoring of Mo(VI) Schiff base complex into SBA-15 as a novel heterogeneous catalyst for enhanced alkene epoxidation

**Jian Zhang[1,2] · Pingping Jiang[1] · Yirui Shen[1] · Weijie Zhang[1] · Gang Bian[1]**

Published online: 17 November 2015


**Abstract** Molybdenum(VI) Schiff base complexes modified mesoporous SBA-15 hybrid heterogeneous catalysts were synthesized by the reaction of $MoO_2(acac)_2$ with mesoporous SBA-15 functionalized by grafting procedures of 3-aminopropyl-triethoxysilane and salicylaldehyde, respectively. The physico-chemical properties of the as-synthesized catalysts were analyzed by ICP-AES, XRD, $N_2$ adsorption–desorption, FT-IR, SEM, TEM and EDX. The as-synthesized catalysts were effective in the catalytic epoxidation of cyclohexene. The catalytic activity can be further enhanced by silylation of the residual Si–OH groups using $Me_3SiCl$, which was largely due to the higher content of Mo active sites. The conversion and selectivity reached to 97.78 and 93.99 % using tert-butyl hydroperoxide as oxidant for Mo–$CH_3$–SA–$NH_2$–SBA-15, while 81.97 and 89.41 % in conversion and selectivity for Mo–SA–$NH_2$–SBA-15. At the same time, the catalytic performances of the hybrid materials were further systematically investigated under various reaction conditions (solvent, oxidants and alkenes, etc.). Mo–$CH_3$–SA–$NH_2$–SBA-15 catalyst can be recycled effectively and reused four cycles with little loss in activity. In addition, the results from hot filtration demonstrated that the catalytic activity mostly resulted from the heterogeneous catalytic process.

✉ Pingping Jiang
ppjiang@jiangnan.edu.cn

[1] The Key Laboratory of Food Colloids and Biotechnology, Ministry of Education, School of Chemical and Material Engineering, Jiangnan University, Wuxi 214122, People's Republic of China

[2] School of Chemistry and Environmental Science, Lanzhou City University, Lanzhou 730070, People's Republic of China

**Keywords** Molybdenum(VI) Schiff base complexes · SBA-15 · Alkene · Epoxidation · Silylation

## 1 Introduction

Alkene epoxidation in the liquid phase is an important industrial reaction in the manufacturing of fine chemicals [1, 2], and most of compounds are valuable intermediates in industry for production of polyethers [3], Cosmetics [4], perfume [5], etc. During these epoxidation reactions, catalyst plays a crucial role and dominates the whole reaction. Therefore, finding an efficient catalyst in the epoxidation of alkenes becomes a hot research field. Homogeneous molybdenum(VI) (Mo(VI)) catalysts are efficient epoxidation catalysts compared with other transition metal catalysts, which thus attracts a considerable interest in the synthesis of novel Mo (VI) complexes for the epoxidation of alkenes. Among the homogeneous molybdenum(VI) catalysts, Mo(VI) Schiff base catalysts has been a hotspot. To date, a variety of Mo(VI) Schiff-base ligands such as bidentate ligands (N,N-dialkylamidinates [6] and N,O-salicylaldiminato [7]), tridentate ligands (O–N–O-salicylaldimine [8–10]) and tetradentate ligands (O–N–N–O-donor [11]) have been used to improve the catalytic activity of these reactions with suitable peroxides. In the case of molybdenum based catalysts derived from Schiff base ligands, dioxomolybdenum species have been particularly investigated because of their good catalytic activity for the selective oxidation of cycloalkenes.

In recent years, the heterogeneous complexes catalysts have received increasing attention due to the disadvantages of homogeneous complexes catalysts, such as poor recyclability and catalyst residues in the products. To remedy for these disadvantages, grafting homogeneous complexes catalysts

onto a support through covalent linkage is a valid solution [12]. Moreover, flexible organic linkages can provide more accessibility to the catalytic center by increasing mobility of the loaded complex [13]. In addition to these features, easy recovery and product separation can be possible by heterogeneous catalysts based on supported Schiff bases complexes [14, 15]. Therefore, heterogenization of homogenous catalysts has attracted immense consideration [16]. The hexagonally ordered mesoporous SBA-15 material was more commonly used as a support comparing with MCM series (MCM-41, MCM-48 and MCM-15) due to its larger pore diameters and pore volumes [17]. In particular, the larger pores for SBA-15 enable immobilization of larger biomolecules, which cannot be accommodated in small pores. To extend the applicability of SBA-15 materials, it is necessary to modify the surface by organic functional groups for anchoring metals and metal complexes. The surface silylation reaction is becoming the most popular way to alter the surface reactivity or to tune other surface properties such as polarity, mechanical compression and hydrophobicity of such materials [18].

In this paper, in order to further enhance catalytic activity than previous works [19], two novel molybdenum(VI) tridentate Schiff base complexes supported onto modified mesoporous SBA-15 were prepared by a covalent grafting method, one of which involved the post-synthesis silylation (Mo–$CH_3$–SA–$NH_2$–SBA-15), the other was not treated by silylation (Mo–SA–$NH_2$–SBA–15). The modification with $Me_3SiCl$ for surface of SBA-15 is expected to enhance catalytic performance. The composition, structure, morphology and textural properties of as-prepared hybrid catalysts were characterized by spectroscopy methods, X-ray diffraction analysis, transmission electron microscopy, EDX spectrum, ICP-AES and nitrogen adsorption–desorption measurement. Subsequently, their catalytic performances were tested by epoxidation of different alkenes, oxidant and solvents. Meanwhile, the contribution of silylation and Schiff base to the overall catalytic oxidation activity of the hybrid catalysts were evaluated and explained. A possible reaction mechanism was proposed. In addition, the catalytic stability and recyclability are discussed in detail. These studies potentially propel the development of novel catalysis materials for epoxidation of alkenes and make it possible to get a deep insight into the relationship between the structure and the catalytic activity by structural interrogation.

## 2 Experimental

### 2.1 Materials

3-aminopropyl-trimethoxysilane (abbreviated as APTES, 98.0 wt%) and salicylaldehyde were purchased from Sinopharm Chemical Reagent Co., Ltd. and without further purification. 50 wt% hydrogen peroxide (Arkema, China), Alkenes and solvents are A.R. grade. SBA-15 was prepared as reported [20], $MoO_2(acac)_2$ was prepared according to previous Ref. [21].

### 2.2 Preparation

The synthesis procedures of Mo–$CH_3$–SA–$NH_2$–SBA-15 are presented in Scheme 1.

#### *2.2.1 Synthesis of $NH_2$–SBA-15*

Amino-functionalized SBA-15 (denoted as $NH_2$–SBA-15) was prepared based on a reported method by Mckittrick and Jones [22]. Briefly, 1.0 g of SBA-15 (pretreated at 120 °C for 2 h) was added to 100 mL of dry toluene in a 250 mL flask. Then 1.0 mL of 3-aminopropyltriethoxysilane (APTES) was added and the mixture stirred at reflux temperature (120 °C) for 24 h. The resulting product was filtrated, washed with toluene and ethanol, and dried in air. Elemental analysis: found C, 4.92; H, 1.51; N, 1.63 %.

#### *2.2.2 Synthesis of SA–$NH_2$–SBA-15*

1.0 g of $NH_2$–SBA-15 and 2 mmol of salicylaldehyde were added in 35 mL of absolute ethanol. The mixture was refluxed at 80 °C for 24 h to obtain a Schiff base ligand complex (marked as SA–$NH_2$–SBA-15). The resulting solid was filtered, Soxhlet extracted with ethanol to remove the unreacted salicylaldehyde, and dried under vacuum at 80 °C overnight [23]. Elemental analysis: found C, 8.37; H, 0.93; N, 0.91 %.

#### *2.2.3 Synthesis of $CH_3$–SA–$NH_2$–SBA-15*

In a typical silylation modification experiment [24, 25], 1.0 g of SA–$NH_2$–SBA-15 was added in a mixture solution of 30 mL of toluene and 1.00 mL (9.2 mmol) of $Me_3SiCl$ and stirred at room temperature for 24 h. The resulting product (labeled as $CH_3$–SA–$NH_2$–SBA-15) was filtered, washed with acetone and ethanol, and dried at 80 °C. Elemental analysis: found C, 9.46; H, 1.35; N, 0.73 %.

#### *2.2.4 Synthesis of Mo–$CH_3$–SA–$NH_2$–SBA-15*

1.0 g of $CH_3$–SA–$NH_2$–SBA-15 was added in 10 mL ethanol and heated to 85 °C. Then 35 mL of ethanol solution containing 0.5 mmol $MoO_2(acac)_2$ was added dropwise under stirring. The mixture was refluxed for 24 h. The resulting product (named as Mo–$CH_3$–SA–$NH_2$–SBA-15) was filtered, Soxhlet extracted with a mixture of dichloromethane and ethanol (volume ratio: 1:1) and dried

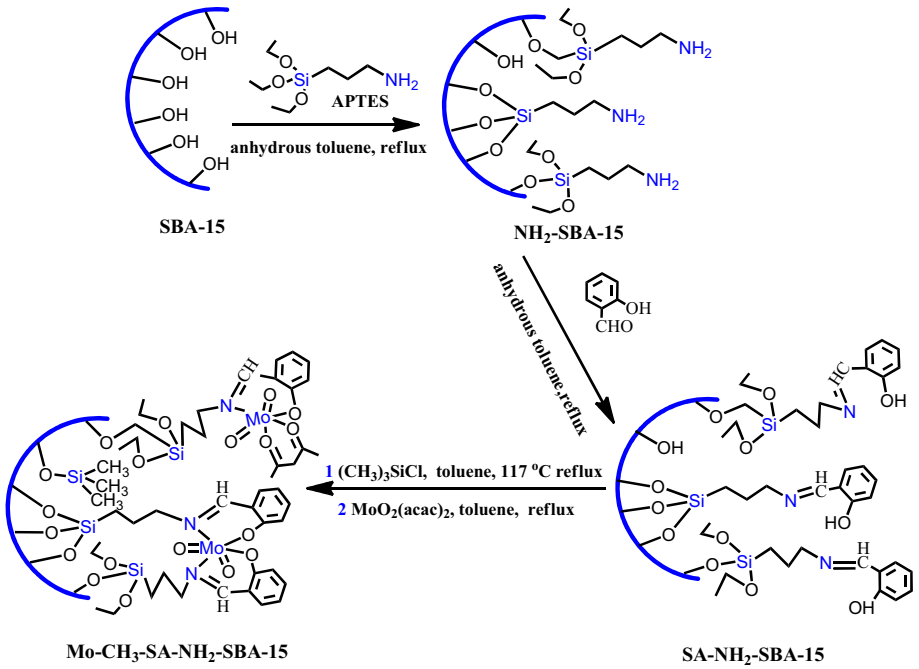


**Scheme 1** Procedures of the synthesis of Mo–$CH_3$–SA–$NH_2$–SBA-15

under vacuum at 80 °C. Elemental analysis: found C, 8.14; H, 1.03; N, 0.65 %.

For comparison, Mo–SA–$NH_2$–SBA-15 was prepared under the same reaction condition without the procedure of silylation modification. Elemental analysis: found C, 6.48; H, 0.81; N, 0.46 %.

### 2.3 Characterization

X-ray diffraction (XRD) patterns of samples were recorded on a Bruker D8 adcanced powder X-ray diffractometer with a Cu Kα radiation source. The surface area and pore size distribution of samples were measured using a Micromeritics ASAP 2020 surface area and porosity analyzer at −196 °C with nitrogen as the analysis gas. Prior to measurement, all samples were degassed at the desired temperature (200 °C for SBA-15, 95 °C for Mo–SA–$NH_2$–SBA-15 and Mo–$CH_3$–SA–$NH_2$–SBA-15) for 5 h. To confirm the morphology and size of the samples, transmission electron microscopy (TEM) micrographs were recorded in a JEM-2100 UHR electron microscope (Japan) with an acceleration voltage of 200 kV and in a Hitachi S-4800 field-emission scanning electron microscope (SEM) with an acceleration voltage of 2 kV. Energy-dispersive X-ray spectroscopy (EDX) was taken on the TEM. The content of molybdenum in samples was determined by a Perkin Elmer AA-300 spectrophotometer (ICP-AES). The infrared spectra (500–4000 $cm^{-1}$) of samples were recorded on a NICOLET 6700 FT-IR Thermoscientific spectrometer employing a KBr disc method.

### 2.4 Catalytic alkene epoxidation

A typical catalytic cyclohexene epoxidation experiment was carried out as follows. 200 mg of catalyst, 10 mL of 1,2-dichloroethane (1,2-DCE), 10 mmol cyclohexene as a substrate and 5 mmol n-octane as internal standard were added in a 25 mL round bottom flask equipped with a reflux condenser. Then 15 mmol of TBHP aqueous solution (65 wt%) was added. The reaction temperature was controlled at 83 °C. Samples were taken at intervals and analyzed by a gas chromatograph (GC, SP-6890A) equipped with a FID detector and a capillary column (SE-54 30 m × 0.32 mm × 0.25 μm). Before analysis, samples need to be centrifuged. The catalytic activity for the epoxidation of cyclohexene was evaluated by the transformation of cyclohexene to cyclohexene epoxide.

## 3 Results and discussion

### 3.1 Structural characteristics

#### *3.1.1 XRD*

The XRD patterns of parent SBA-15, Mo–SA–$NH_2$–SBA-15 and Mo–$CH_3$–SA–$NH_2$–SBA-15 were presented in Fig. 1. As shown, three obvious diffraction peaks were observed in the small angle XRD patterns of parent SBA-15 (Fig. 1a). Among them, the strongest peak with 2θ value between 0.9° and 1.2° corresponded to (100) reflection. The other two peaks between 1.5° and 2.0° corresponded to

(110) and (200) reflections, respectively. These peaks were ascribed to the order hexagonal unit cell of the typical SBA-15 materials. Similar to SBA-15, Mo–SA–$NH_2$–SBA-15 and Mo–$CH_3$–SA–$NH_2$–SBA-15 (Fig. 1b and 1c, respectively) also have three diffraction peaks between 0.9° and 2.0° but with lower intensity and shift to small angle, which was due to decrease in the mesoscopic order and high contrast matching between the silicate wall and Mo(VI) Schiff base located inside the SBA-15 pores. However, Mo–$CH_3$–SA–$NH_2$–SBA-15 showed the lower peak intensity and more shift in comparison with Mo–SA–$NH_2$–SBA-15, which was largely resulted from more Mo(VI) Schiff base ligand groups incorporated in the pores of SBA-15 for Mo–$CH_3$–SA–$NH_2$–SBA-15 than Mo–SA–$NH_2$–SBA-15 [26].

### 3.1.2 Nitrogen sorption

The nitrogen adsorption–desorption isotherms and the corresponding pore size distribution (the inset) of parent SBA-15, Mo–SA–$NH_2$–SBA-15 and Mo–$CH_3$–SA–$NH_2$–SBA-15 were displayed in Fig. 2. As shown, all materials were found to maintain a type IV isotherm with H1 hysteresis loop (appeared at $P/P_0 = 0.5$–$0.80$) corresponding to capillary condensation of nitrogen gas in the typical mesoporous materials [27]. This result indicated that the modification surface modification of Mo(VI) Schiff base hardly change the mesoporous nature of SBA-15. However, the hysteresis loops for both Mo–SA–$NH_2$–SBA-15 and Mo–$CH_3$–SA–$NH_2$–SBA-15 showed the shift to low *P*/*P*o value, which was because the surface modification of Mo(VI) Schiff base tended to decrease the pore size of SBA-15. More shifts were found for Mo–$CH_3$–SA–$NH_2$–SBA-15 relative to Mo–SA–$NH_2$–SBA-15 indicating the smaller size of pore distribution for Mo–$CH_3$–SA–$NH_2$–SBA-15 than Mo–SA–$NH_2$–SBA-15. This was due to more Mo(VI) Schiff ligand groups base incorporated in the pores

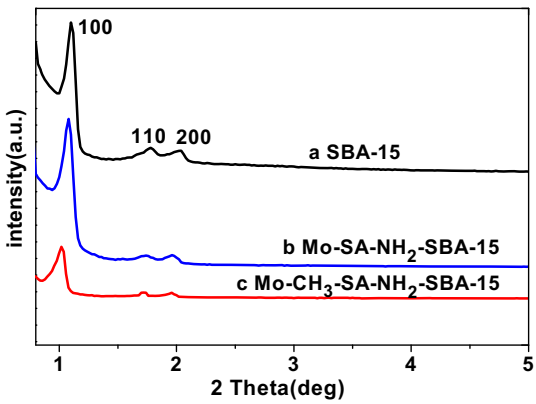


**Fig. 1** XRD patterns of *a* SBA-15, *b* Mo–SA–$NH_2$–SBA-15, *c* Mo–$CH_3$–SA–$NH_2$–SBA-15

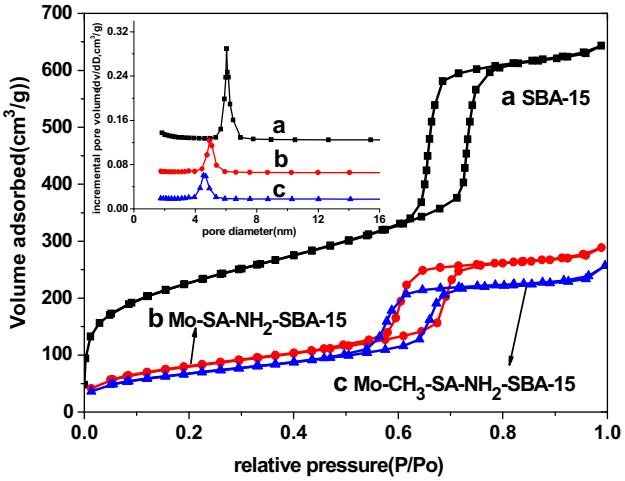


**Fig. 2** $N_2$ adsorption–desorption isotherms and pore size distribution profiles (*inset*) of various materials. *a* SBA-15, *b* Mo–SA–$NH_2$–SBA-15, *c* Mo–$CH_3$–SA–$NH_2$–SBA-15

of SBA-15 for Mo–$CH_3$–SA–$NH_2$–SBA-15. The inset of Fig. 2 showed the pore size distributions of parent SBA-15, Mo–SA–$NH_2$–SBA-15 and Mo–$CH_3$–SA–$NH_2$–SBA-15. They were in the range of 5.2–7.0, 4.0–5.8 and 3.7–5.4 nm, respectively.

Table 1 summarized the textural characteristics of SBA-15, Mo–SA–$NH_2$–SBA-15 and Mo–$CH_3$–SA–$NH_2$–SBA-15. The BET specific surface areas ($S_{BET}$), total pore volume ($V_{BJH}$) and average pore diameter ($D_{BJH}$) of the parent SBA-15 were 793 $m^2/g$, 0.78 $cm^3/g$ and 5.9 nm. Compared with parent SBA-15, Mo–SA–$NH_2$–SBA-15 and Mo–$CH_3$–SA–$NH_2$–SBA-15 exhibited lower $S_{BET}$ (288 and 244 $m^2/g$, respectively), $V_{BJH}$ (0.41 and 0.37 $cm^3/g$, respectively) and $D_{BJH}$ (5.6 and 5.5 nm). At the same time, in comparison with Mo–SA–$NH_2$–SBA-15, Mo–$CH_3$–SA–$NH_2$–SBA-15 showed lower $S_{BET}$, $V_{BJH}$ and $D_{BJH}$ which was probably due to a high quantity of grafted complex in the Mo–$CH_3$–SA–$NH_2$–SBA-15.

In order to evaluate the amount of Mo(VI) Schiff base ligand groups, the contents of molybdenum in Mo–SA–$NH_2$–SBA-15 and Mo–$CH_3$–SA–$NH_2$–SBA-15 were determined by ICP-AES (Table 1). They are 0.466 and 0.625 mmol/g, respectively. Clearly, Mo–$CH_3$–SA–$NH_2$–

**Table 1** Textural properties of the samples

| Sample | Mo content[a] | $S_{BET}$ | $V_{BJH}$ | $D_{BJH}$ |
|---|---|---|---|---|
| SBA-15 | – | 793 | 0.78 | 5.9 |
| Mo–SA–$NH_2$–SBA-15 | 0.466 | 288 | 0.41 | 5.6 |
| Mo–$CH_3$–SA–$NH_2$–SBA-15 | 0.625 | 244 | 0.37 | 5.5 |

Specific surface area, $S_{BET}(m^2\ g^{-1})$; pore volume, $V_{BJH}(cm^3\ g^{-1})$; pore diameter, $D_{BJH}$(nm)

[a] From ICP-AES analysis, mmol/g

SBA-15 had more Mo(VI) Schiff base ligand groups as active sites for increased catalytic activity. This result could be explained by the silylation modification in the preparation of Mo–$CH_3$–SA–$NH_2$–SBA-15 which helped to immobilize more Mo(VI) Schiff base ligand groups on SBA-15 matrix accessibly.

#### *3.1.3 SEM, TEM and EDX*

Figure 3a, d depicted the SEM images for SBA-15 and Mo–$CH_3$–SA–$NH_2$–SBA-15, respectively. Both SBA-15 and Mo–$CH_3$–SA–$NH_2$–SBA-15 presented similar noodle-like morphologies, which indicated that silylation modification and Mo(VI) Schiff base ligand groups graft seemed to scarcely undermine the morphology of SBA-15 support. Figure 3b, c, e and f showed TEM images of SBA-15 and Mo–$CH_3$–SA–$NH_2$–SBA-15. Compared with SBA-15 (Fig. 3b), Mo–$CH_3$–SA–$NH_2$–SBA-15 maintained the hexagonal structure (Fig. 3e). However, more coarse feature was observed on the surface of Mo–$CH_3$–SA–$NH_2$–SBA-15 in comparison with SBA-15 (Fig. 3c, f), which was mostly due to the formation of Mo(VI) Schiff base ligand groups graft on the surface. The energy dispersive X-ray spectrometry (EDX) spectrum in Fig. 3g showed the existence of elements Si, O, N, C, Mo and Cu. The signals of partial C and Cu came from the TEM copper grid [28]. The EDX analysis result (the inset) revealed the molar ratio of N to Mo was ca. 1.4:1.3, which was close to the theory ratio of 1:1, indicating that almost all of the Schiff bases coordinated with Mo(VI).

#### *3.1.4 FT-IR*

Figure 4 presented the FT-IR spectra of SBA-15, Mo–SA–$NH_2$–SBA-15 and Mo–$CH_3$–SA–$NH_2$–SBA-15. As shown, SBA-15 showed bands at approximately 1082 and 805 $cm^{-1}$ assigned to characteristic vibrations of the mesoporous framework (Si–O–Si). The peaks at 3464 and 1634 $cm^{-1}$ were assigned to stretching and bending vibrations of surface Si–OH groups of the supported SBA-15 surface. And Si–OH stretch ($\nu_{Si-OH}$) at 960 $cm^{-1}$ was observed in the FT-IR spectra of all samples [29, 30]. For synthesized Mo–SA–$NH_2$–SBA-15, the appearance of new peaks at 2943 $cm^{-1}$ attributed to C–H asymmetric stretching ($\nu_{as}$(–C–H)). The C=N bending vibration (ν(–C = N)) at 1634 $cm^{-1}$ was overlapped with the vibrations attributed to ν(–OH). The $\nu_s$(Mo=O) vibration of complex appeared around 963 $cm^{-1}$ [31, 32], which overlaps with the $\nu_{Si-O}$ of Si–OH groups. And the asymmetric stretching vibrations of Mo=O was appeared at 904 $cm^{-1}$. Compared with Mo–SA–$NH_2$–SBA-15, the IR spectra of Mo–$CH_3$–SA–$NH_2$–SBA-15 appeared a new peak at 1394 $cm^{-1}$ attributed to the –$CH_3$ bending vibration (δ(–$CH_3$)) from $Si(CH_3)_3$− groups, at 688 and 611 $cm^{-1}$ attributed to the Si–$CH_3$ asymmetric stretching ($\nu_{as}$ (Si–C)) and symmetric stretching ($\nu_s$(Si–C)) [33], which proved the binding of chlorotrimethylsilane molecules to the surface of SBA-15. The results obtained from FT-IR spectra confirm the successful silylation of organosilanes on SBA-15.

### 3.2 Catalytic epoxidation of alkenes

The catalytic activity of Mo–$CH_3$–SA–$NH_2$–SBA-15 and Mo–SA–$NH_2$–SBA-15 was evaluated through the epoxidation reaction of cyclohexene using TBHP as an oxidant (Fig. 5). As expected, both samples showed catalytic activities and high selectivities. In the reaction time of 13 h, the conversion and selectivity of cyclohexene increased to 97.78 and 93.99 % for Mo–$CH_3$–SA–$NH_2$–SBA-15, and 81.97 and 89.41 % for Mo–SA–$NH_2$–SBA-15. Compared with Mo–SA–$NH_2$–SBA-15, Mo–$CH_3$–SA–$NH_2$–SBA-15 presented higher catalytic epoxidation activity and selectivity. These results were consistent with the reported study that the silylation treatment could make catalyst surface become more hydrophobic by decreasing of the number of surface Si–OH groups, thus improving accessibility to the substrate and oxidant species due to their hydrophobic property [18].

In epoxidation reactions, solvent usually plays an important role and can also affect the conversion and selectivity of products [34]. Therefore, the influence of different solvents on the oxidation of cyclohexene was studied using Mo–$CH_3$–SA–$NH_2$–SBA-15 and the results were summarized in Tables 2. Among 1,2-dichloroethane (1,2-DCE), acetonitrile, ethyl acetate and ethanol solvents, the highest conversion and selectivity were obtained in 1,2-DCE, while the low conversion and selectivity were observed in ethanol, ethyl acetate and acetonitrile solvents. In generally, TBHP was coordinated with the molybdenum(VI) center and then oxygen transition can be occurred to the substrate. However, once the strong p-donor organic solvent is capable of coordinating with the molybdenum center, the coordination between oxygen and Mo(VI) center will decrease. As the coordination ability of the solvent increased, the coordination of the solvent with Mo(VI) become easier, which will inhibit the TBHP coordination and retards the reaction progress, resulting in the decrease of the epoxide yield. Due to the presence of oxygen atoms with a long electron pair, acetonitrile, ethyl acetate and ethanol solvents could effectively compete with TBHP to bind to the Mo(VI) center and inhibited the epoxidation reaction [35, 36]. Therefore, there is a low conversion and selectivity observed in ethanol, ethyl acetate and acetonitrile solvents [37–40]. However, the difference in selectivity about 1,2-DCE may be due to the electronic effect of chlorine, which would increase the

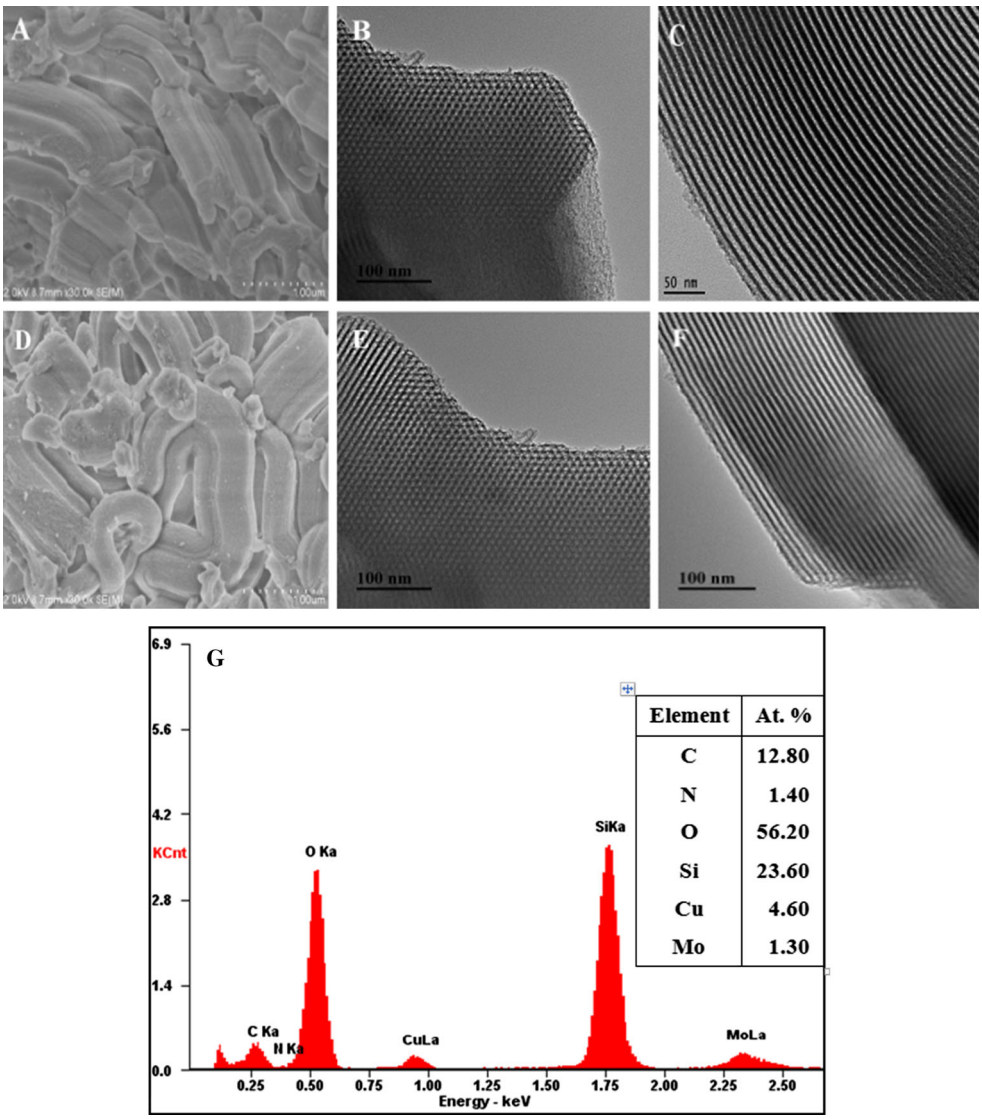


**Fig. 3** SEM and TEM images at different magnifications. (**a**, **d** for SEM of SBA-15 and Mo–$CH_3$–SA–$NH_2$–SBA-15, respectively; **b**, **c** for TEM of SBA-15 and **e**, **f** for TEM of Mo–$CH_3$–SA–$NH_2$–SBA-15, respectively.); **g** EDX spectrum of Mo–$CH_3$–SA–$NH_2$–SBA-15 (*inset*: atomic percentages of C, N, O, Si, Cu and Mo)

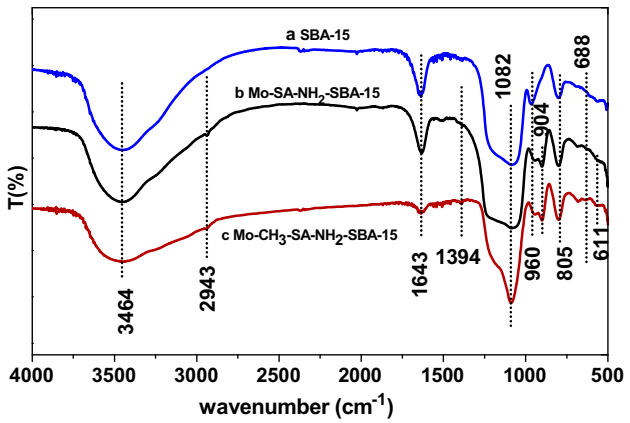


**Fig. 4** FT-IR spectrum of *a* SBA-15; *b* Mo–SA–$NH_2$–SBA-15; *c* Mo–$CH_3$–SA–$NH_2$–SBA-15

selectivity in heterogeneous epoxidation. It is apparent that chlorine of 1,2-DCE led to significant enhancement of selectivity. It has been also reported that chlorine is the most powerful promoter for selectivity of alkene [41, 42].

To evaluate the effects of oxidations, the effects of several common oxidants (such as TBHP, $H_2O_2$, $O_2$) were studied in the oxidation of cyclohexene and the results were demonstrated in Fig. 6. In the reaction of 6 h, the conversion and selectivity were 78.47 and 93.90 %, 49.03 and 55.70 %, and 36.27 and 26.65 % for TBHP, $H_2O_2$ and $O_2$, respectively. Evidently, the highest catalytic performance was obtained for TBHP, which was largely because of the effective contact with Mo–$CH_3$–SA–$NH_2$–SBA-15 to form the intermediate complex to catalytic epoxidation of alkenes and transfer oxygen to alkenes. Molecular

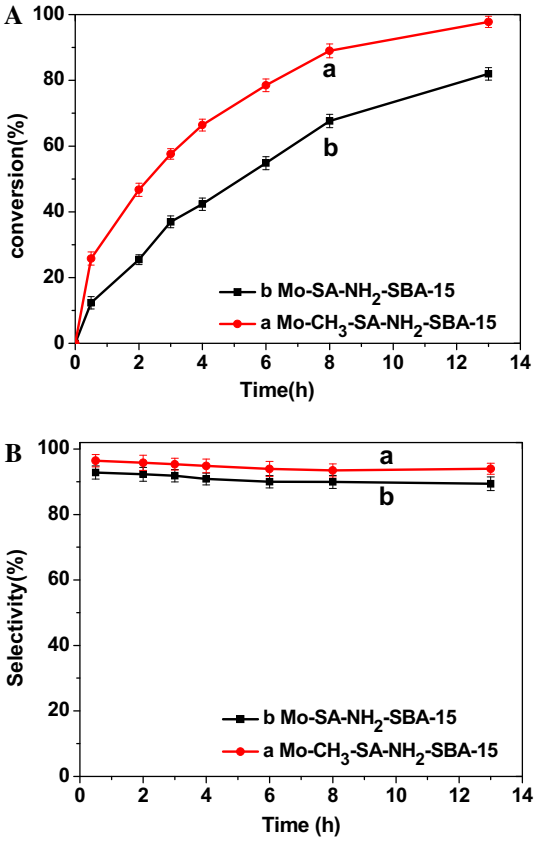


**Fig. 5** Epoxidation conversion (**a**) and selectivity (**b**) of cyclohexene with catalyst *a* Mo–$CH_3$–SA–$NH_2$–SBA-15, *b* Mo–SA–$NH_2$–SBA-15, the reaction condition: catalyst (200 mg), cyclohexene (10 mmol), TBHP (15 mmol), temperature 83 °C, and solvent: 1,2-dichloroethane(1,2-DCE) (10 ml), internal standard: n-octane(5 mmol). Determined by GC, the product of cyclohexene epoxide, and the byproducts 2-cyclohexene-1-ol, 1,2-cyclohexenediol and 2-cyclohexene-1-one were acquired

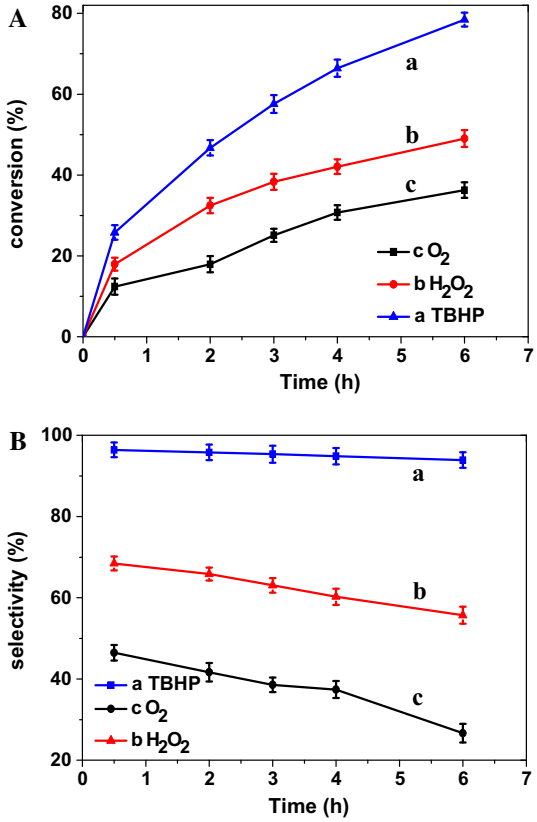


**Fig. 6** Epoxidation of cyclohexene with different oxidants catalyzed by Mo–$CH_3$–SA–$NH_2$–SBA-15. *a* TBHP, *b* 50wt% $H_2O_2$, *c* $O_2$. Reaction conditions: cyclohexene (10 mmol), oxidant (15 mmol, liquid oxidation; $O_2$ for 10 mL/min, in open system (1 atm)), 1,2-DCE (10 ml), n-octane (5 mmol) as internal standard, catalyst (200 mg), reaction temperature (83 °C). Determined by GC, the product of cyclohexene epoxide, and the byproducts 2-cyclohexene-1-ol, 1,2-cyclohexenediol and 2-cyclohexene-1-one were acquired

**Table 2** The effect of various solvents on the epoxidation of cyclohexene with TBHP

| Entry | Solvent | Conversion (%) | | Selectivity (%) | |
|---|---|---|---|---|---|
| | | 4 h | 8 h | 4 h | 8 h |
| 1 | 1,2-dichloroethane | 57.59 | 88.97 | 94.86 | 93.49 |
| 2 | Acetonitrile | 42.34 | 64.25 | 84.32 | 79.75 |
| 3 | Ethyl acetate | 35.31 | 43.78 | 70.08 | 64.72 |
| 4 | Ethanol | 23.18 | 37.39 | 59.49 | 60.45 |

Reaction conditions: cyclohexene (0.82 g, 10 mmol), TBHP (2.077 g, 15 mmol), catalyst (200 mg), solvent (10 mL), n-octane (0.52 g, 5 mmol, internal standard), temperature: T = 83 °C, reaction times: t = 4 h and 8 h. Determined by GC, the product of cyclohexene epoxide, and the byproducts 2-cyclohexene-1-ol, 1,2-cyclohexenediol and 2-cyclohexene-1-one were acquired

oxygen is not a viable alternative, because it generally leads to non-selective autoxidation [43]. Furthermore, the strong oxidation and higher activity of $O_2$ and $H_2O_2$ would lead to fierce reaction, which may make the epoxide products continue to react and the byproduct formed. Whereas, as an organic oxidate, TBHP owned a moderate property and hardly caused side reaction. Therefore using TBHP as an oxidate can obtain a higher selectivity than $O_2$ and $H_2O_2$ [44, 45].

In order to establish the general applicability of the method, this study was further extended to the catalytic epoxidation of several linear and cyclic alkenes with Mo–$CH_3$–SA–$NH_2$–SBA-15. Figure 7 presented the effects of different alkenes on catalytic epoxidation. As shown, the conversion increased in the order of cyclohexene > cyclooctene > limonene > indene > 1-hexene > 1-octene. In the reaction time of 13 h, the conversion were 97.78, 84.52, 78.41, 71.81, 64.29 and 53.81 %, respectively. 1-hexene, indene, 1-octene showed a lower reactivity than cyclohexene, cyclooctene and limonene, which probably were due to the presence of larger steric hindrances. In addition, cyclohexene, cyclooctene, 1-hexene, 1-octene gave a higher selectivity

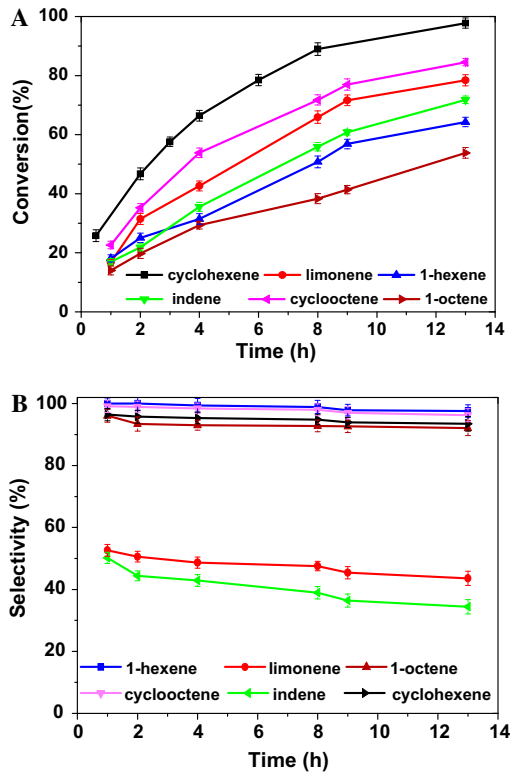


**Fig. 7** epoxidation of different alkenes **a** conversion, **b** selectivity. *a* cyclohexene, *b* cyclooctene, *c* 1-hexene, *d* 1-octene, *e* limonene b, *f* indene. Reaction conditions: alkene(substrate) (10 mmol), TBHP (15 mmol), catalyst (200 mg) and 1,2-dichloroethane (10 mL), n-octane (5 mmol, as internal standard), reaction temperature (83 °C). GC yield based on starting alkene, determined by GC–MS, the product of epoxide, alcohols were produced as byproducts

(above 90 %) than that for limonene and indene. This may be mainly caused by the more sensitivity of the oxide of limonene and indene towards hydrolysis [46]. From Fig. 7b, cyclohexene, cyclooctene, 1-hexene and 1-octene were catalytically oxygenated with high selectivity because of the adjacent donating electron group of epoxidate group. However, due to conjugated effect and electron-withdrawing group linking with neighbour group, the epoxidation of limonene and indene was unstable and easy to produce byproduct. The epoxidation of limonene is more challenging as the substrate includes two different alkenes moieties-one internal and one terminal double bond [10]. After 13 h, only 1,2-epoxy-limonene and 8,9-epoxide-limonene (78.41 %) are obtained as products. The reactions of indene were partly selective to the corresponding epoxide, resulting in the generation of several byproducts including cis-diol, trans-diol and indan-2-one(trace).

To further explain the effect of solvent and oxidant in the epoxidation reaction, based on the reported references [37, 38, 47–49], a reactive pathway for this catalytic reaction was proposed using cyclohexene as the model (Scheme 2). When the addition of TBHP across one terminal Mo=O group, the O–O-t-Bu group of TBHP is end-on bound to molybdenum, with the β oxygen (next to the tert-butyl group) involved in a hydrogen bond with the neighboring OH. The α oxygen (attached to the Mo atom) is transferred to the alkene, producing the epoxide under concomitant elimination of tert-butanol, yielding the initial complex [50]. In this process, the solvent also competes with TBHP for coordination to the molybdenum center and retards the TBHP to coordinate with Mo(VI). When the solvent has lone pair electrons, like O, N can coordinate with Mo and inhibit the TBHP to coordinate. Therefore, reaction of an alkene as a nucleophile with oxygen as an electrophile easily explains the observation that electron rich alkenes react faster than electron poor alkenes.

### 3.3 Recoverability and stability

It is very important to keep the hybrid catalyst with little leakage of the active components and unchangeable catalytic activity in cycle experiments. To assess the long-term stability and reusability of Mo–$CH_3$–SA–$NH_2$–SBA-15, four recycle experiments were carried out in epoxidation of cyclohexene. Each cycle experiment continued 6 h. The used catalyst was recovered by filtration, washed thoroughly with dichloromethane and then dried in 80 °C. The results are showed in Fig. 8. In the first run, the conversion of epoxidation was 78.47 %. After four runs, though Mo–$CH_3$–SA–$NH_2$–SBA-15 showed a slight decrease of catalytic activity, the conversion of cyclohexene was still over 70.56 % indicating the good stability and recoverability of Mo–$CH_3$–SA–$NH_2$–SBA-15. The contents of Mo before and after four runs were determined to evaluate the leaching of Mo(VI) Schiff base ligand groups from Mo–$CH_3$–SA–$NH_2$–SBA-15 surface. After four runs, a few loss amount of Mo (about 8.4 μmol/g) determined for Mo–$CH_3$–SA–$NH_2$–SBA-15 indicated the good structure stability of Mo–$CH_3$–SA–$NH_2$–SBA-15. However, under the same condition, about a total amount of Mo (about 17.3 μmol/g) was lost for Mo–SA–$NH_2$–SBA-15 which higher than that for Mo–$CH_3$–SA–$NH_2$–SBA-15. These results further confirmed that the silylation modification in preparation of Mo–$CH_3$–SA–$NH_2$–SBA-15 enhanced the bond with Mo(VI) Schiff base ligand groups and inhibited the leaching of Mo(VI).

To evaluate the possible effects of leaching of Mo(VI) Schiff base ligand groups, a controlled hot filtration experiment was conducted. After reactions were initiated for 3 h, the cyclohexene conversions were 57.59 % for Mo–$CH_3$–SA–$NH_2$–SBA-15, then, the reaction mixtures were filtered and restarted the reaction on filtrate under the same conditions for another 10 h. Ultimately, the conversions were 61.32 % with a low increment of 3.73 %

**Scheme 2** Proposed mechanism for epoxidation of cyclohexene with TBHP catalyzed by Mo–$CH_3$–SA–$NH_2$–SBA-15

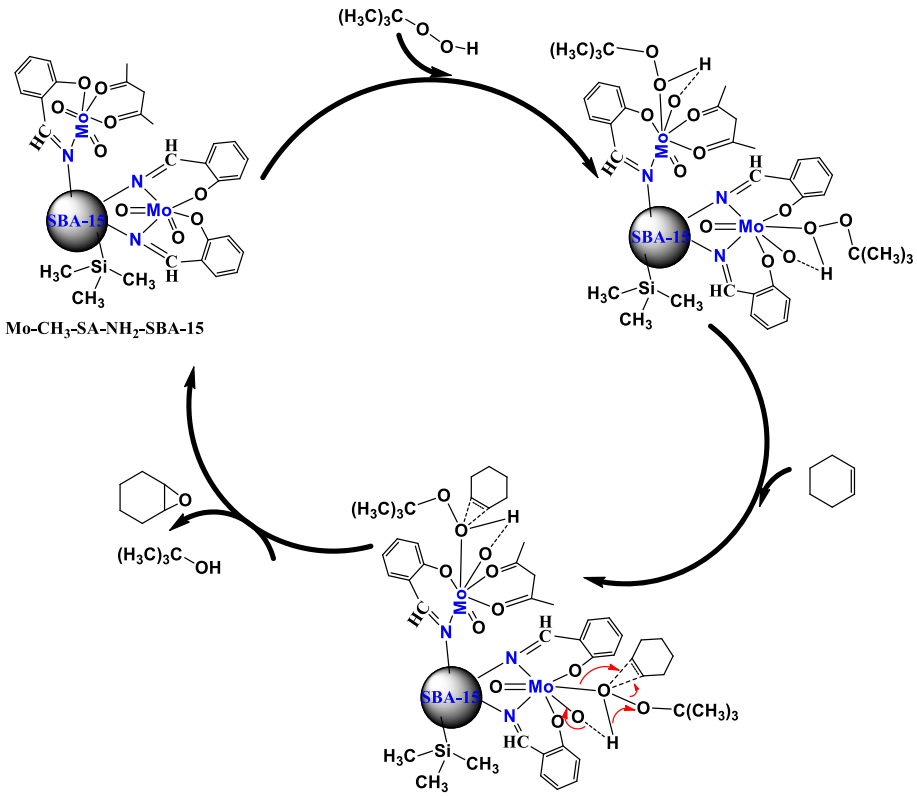


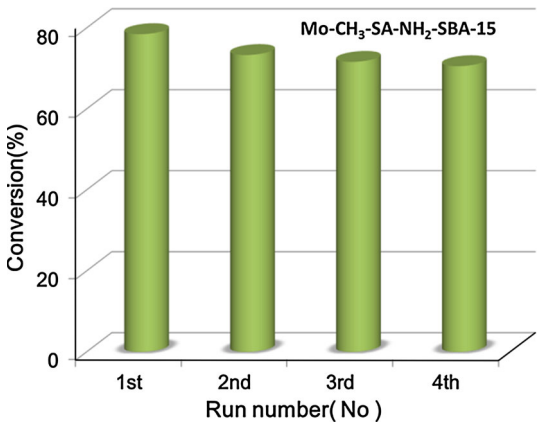


**Fig. 8** Evaluation of the recyclability of Mo–$CH_3$–SA–$NH_2$–SBA-15 material towards the cyclohexene epoxidation reaction. Catalytic activity for the 1st, 2nd, 3rd and 4th run. Each run condition: catalyst amount 200 mg; 1,2-DCE 10 mL; cyclohexene 10 mmol; TBHP 15 mmol; n-octane 5 mmol; 83 °C; 11 h. Determined by GC, the product of cyclohexene epoxide, and the byproducts 2-cyclohexene-1-ol, 1,2-cyclohexenediol and 2-cyclohexene-1-one were acquired

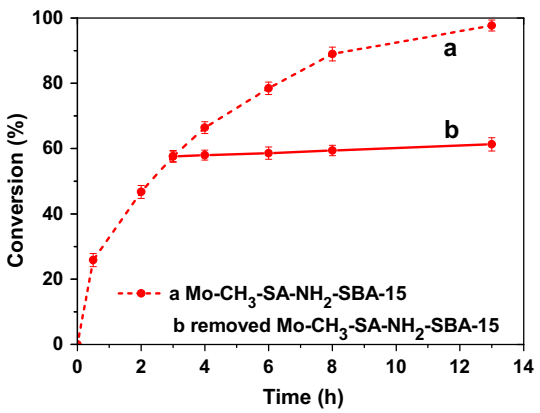


**Fig. 9** *a* The plot of time against conversion for epoxidation of cyclohexene. *b* Heterogeneous reaction check by continuing the reaction after removing the catalyst after 6 h. Reaction conditions: 10 mmol of cyclohexene, 10 ml of 1,2-DCE, 5 mmol of n-octane, 200 mg of catalyst (*a*, Mo–$CH_3$–SA–$NH_2$–SBA-15; *b*, removed the Mo–$CH_3$–SA–$NH_2$–SBA-15), TBHP 15 mmol, temperature 83 °C. Determined by GC, the product of cyclohexene epoxide, and the byproducts 2-cyclohexene-1-ol, 1,2-cyclohexenediol and 2-cyclohexene-1-one were acquired

(Fig. 9). Compared with cyclohexene epoxidation in the presence of Mo–$CH_3$–SA–$NH_2$–SBA-15, it is found that cyclohexene could just be converted at a very low rate when Mo–$CH_3$–SA–$NH_2$–SBA-15 was removed and this trend was even almost parallel with time axle. It is implied that the catalytic activity mostly resulted from the heterogeneous catalytic reaction.

## 4 Conclusions

In conclusion, Mo–SA–$NH_2$–SBA-15 and Mo–$CH_3$–SA–$NH_2$–SBA-15 were realized by a grafting method, which were effective heterogeneous catalysts for the epoxidation.

The results showed that the silylated Mo–$CH_3$–SA–$NH_2$–SBA-15 was more active than Mo–SA–$NH_2$–SBA-15 without silylation due to a high quantity of grafted complex in the Mo–$CH_3$–SA–$NH_2$–SBA-15. A 97.78 % conversion and 93.99 % selectivity of the cyclohexene was achieved after 13 h of reaction when catalyzed by Mo–$CH_3$–SA–$NH_2$–SBA-15. A proposed mechanism for epoxidation was shown that the process of epoxidation and clarified some effective factors in epoxidation. Recycling results of catalyst Mo–$CH_3$–SA–$NH_2$–SBA-15 showed good recoverability without significant loss of activity and selectivity within successive four runs. Hot filtration test were strongly evidenced for a real heterogeneous catalysis and indicated that the undesired slight leaching of the Mo(VI) can be inhibited by silylation treatment.

**Acknowledgments** Thanks for the Fund by the Innovation Foundation in Jiangsu Province of China (BY2014023-08) and the National ''Twelfth Five-Year'' Plan for Science & Technology (2012BAD32B03).

## References

1. T. Punniyamurthy, S. Velusamy, J. Iqbal, Chem. Rev. **105**, 2329 (2005)
2. Q.H. Xia, H.Q. Ge, C.P. Ye, Z.M. Liu, K.X. Su, Chem. Rev. **105**, 1603 (2005)
3. F. Cavani, J.H. Teles, ChemSusChem **2**, 508 (2009)
4. G. Sienel, R. Rieth, K.T. Rowbottom, Ullmann's Encycl. Ind. Chem. **13**, 139 (2000)
5. K. Bauer, D. Garbe, H. Surburg, *Common Fragrance and Flavor Materials: Preparation, Properties and Uses*, vol. 4 (Wiley, NewYork, 2001), pp. 167–226
6. M.P. Coles, R.F. Jordan, J. Am. Chem. Soc. **119**, 8125 (1997)
7. P.A. Cameron, V.C. Gibson, C. Redshaw, J.A. Segal, A.J.P. White, D.J. Williams, J. Chem. Soc. Dalton Trans. **3**, 415 (2002)
8. A. Rezaeifard, M. Jafarpour, H. Raissi, M. Alipour, H. Stoeckli-Evans, Z. Anorg, Allg. Chem. **638**, 1023 (2012)
9. M. Bagherzadeh, M. Zare, M. Amini, T. Salemnoush, S. Akbayrak, S. Özkar, J. Mol. Catal. A Chem. **395**, 470 (2014)
10. M. Bagherzadeh, M. Zare, T. Salemnoush, S. Özkar, S. Akbayrak, Appl. Catal. A Gen. **475**, 55 (2014)
11. S.M. Bruno, S.S. Balula, A.A. Valente, F.A. Almeida Paz, M. Pillinger, C. Sousa, J. Klinowski, C. Freire, P. Ribeiro-Claro, I.S. Gonçalves, J. Mol. Catal. A Chem. **270**, 185 (2007)
12. D. Choudhary, S. Paul, R. Gupta, J.H. Clark, Green Chem. **8**, 479 (2006)
13. B. Karimi, A. Zamani, J.H. Clark, Organometallics **24**, 4695 (2005)
14. M. Selvaraj, V. Narayanan, S. Kawi, Micropor. Mesopor. Mater. **132**, 494 (2010)
15. N. Malumbazo, S.F. Mapolie, J. Mol. Catal. A Chem. **312**, 70 (2009)
16. S. Minakata, M. Komatsu, Chem. Rev. **109**, 711 (2008)
17. V. Meynen, P. Cool, E.F. Vansant, Micropor. Mesopor. Mater. **125**, 170 (2009)
18. S.M. Bruno, J.A. Fernandes, L.S. Martins, I.S. Gonçalves, M. Pillinger, P. Ribeiro-Claro, J. Rocha, A.A. Valente, Catal. Today **114**, 263 (2006)
19. J. Zhang, P. Jiang, Y. Shen, W. Zhang, X. Li, Micropor. Mesopor. Mater. **206**, 161 (2015)
20. D. Zhao, J. Feng, Q. Huo, N. Melosh, G.H. Fredrickson, B.F. Chmelka, G.D. Stucky, Science **279**, 548 (1998)
21. M.M. Jones, J. Am. Chem. Soc. **81**, 3188 (1959)
22. M.W. McKittrick, C.W. Jones, Chem. Mater. **17**, 4758 (2005)
23. M. Masteri-Farahani, F. Farzaneh, M. Ghandi, J. Mol. Catal. A Chem. **248**, 53 (2006)
24. M. Jia, A. Seifert, W.R. Thiel, Chem. Mater. **15**, 2174 (2003)
25. C.D. Nunes, M. Pillinger, A.A. Valente, J. Rocha, A.D. Lopes, I.S. Gonçalves, Eur. J. Inorg. Chem. **2003**, 3870 (2003)
26. L. Song, T. Bu, L. Zhu, Y. Zhou, Y. Xiang, D. Xia, J. Phys. Chem. C **118**, 9468 (2014)
27. X. Zhang, S. Liu, H. Tong, G. Yong, Appl. Catal. B Environ. **127**, 105 (2012)
28. J. Luo, H.T. Zhu, H.M. Fan, J.K. Liang, H.L. Shi, G.H. Rao, J.B. Li, Z.M. Du, Z.X. Shen, J. Phys. Chem. C **112**, 12594 (2008)
29. C.D. Nunes, A.A. Valente, M. Pillinger, J. Rocha, I.S. Gonçalves, Chem. Eur. J. **9**, 4380 (2003)
30. F. Balas, M. Manzano, P. Horcajada, M. Vallet-Regí, J. Am. Chem. Soc. **128**, 8116 (2006)
31. M. Bagherzadeh, M. Amini, A. Ellern, L.K. Woo, Inorg. Chem. Commun. **15**, 52 (2012)
32. N. Gharah, S. Chakraborty, A.K. Mukherjee, R. Bhattacharyya, Inorg. Chim. Acta **362**, 1089 (2009)
33. Y. Song, Y. Huang, E.A. Havenga, I.S. Butler, Vib. Spectrosc. **27**, 127 (2001)
34. H. Alper, M. Harustiak, J. Mol. Catal. A Chem. **84**, 87 (1993)
35. F.E. Kühn, M. Groarke, É. Bencze, E. Herdtweck, A. Prazeres, A.M. Santos, M.J. Calhorda, C.C. Romão, I.S. Gonçalves, A.D. Lopes, Chem. Eur. J. **8**, 2370 (2002)
36. M. Minelli, J.H. Enemark, R.T.C. Brownlee, M.J. O'connor, A.G. Wedd, Coordin. Chem. Rev. **68**, 169 (1985)
37. S. Rayati, N. Rafiee, A. Wojtczak, Inorg. Chim. Acta **386**, 27 (2012)
38. Y. Li, X. Fu, B. Gong, X. Zou, X. Tu, J. Chen, J. Mol. Catal. A Chem. **322**, 55 (2010)
39. M. Bagherzadeh, R. Latifi, L. Tahsini, V. Amani, A. Ellern, L. Keith Woo, Polyhedron **28**, 2517 (2009)
40. K. Ambroziak, R. Pelech, E. Milchert, T. Dziembowska, Z. Rozwadowski, J. Mol. Catal. A Chem. **211**, 9 (2004)
41. R.M. Lambert, R.L. Cropley, A. Husain, M.S. Tikhov, Chem. Commun. **10**, 1184 (2003)
42. R.M. Lambert, F.J. Williams, R.L. Cropley, A. Palermo, J. Mol. Catal. A Chem. **228**, 27 (2005)
43. I. Arends, R.A. Sheldon, Top. Catal. **19**, 133 (2002)
44. S.-C. Chua, X. Xu, Z. Guo, Process Biochem. **47**, 1439 (2012)
45. P. Visuvamithiran, K. Shanthi, M. Palanichamy, V. Murugesan, Catal. Sci. Technol. **3**, 2340 (2013)
46. M.C.A. van Vliet, I.C.E. Arends, Chem. Commun. **9**, 821 (1999)
47. M.E. Judmaier, C. Holzer, M. Volpe, N.C. Mosch-Zanetti, Inorg. Chem. **51**, 9956 (2012)
48. M. Bagherzadeh, M. Zare, V. Amani, A. Ellern, L. Keith Woo, Polyhedron **53**, 223 (2013)
49. W.R. Thiel, T. Priermeier, Angew. Chem. Int. Edit. **34**, 1737 (1995)
50. P.J. Costa, M.J. Calhorda, F.E. Kühn, Organometallics **29**, 303 (2009)